

Effect of Compatibilization on the Properties of HIPS/PA1010 Blends

GUANGXIN CHEN, JINGJIANG LIU

Polymer Physics Laboratory, Changchun Institute of Applied Chemistry, Chinese Academy of Sciences, Changchun, 130022, People's Republic of China

Received 11 January 1999; accepted June 5, 1999

ABSTRACT: Blends consisting of high-impact polystyrene (HIPS) as the matrix and polyamide 1010 (PA1010) as the dispersed phase were prepared by mixing. The grafting copolymers of HIPS and maleic anhydride (MA), the compatibilizer precursors of the blends, were synthesized. The contents of the MA in the grafting copolymers are 4.7 wt % and 1.6 wt %, and were assigned as HAM and LMA, respectively. Different blend morphologies were observed by scanning electron microscopy (SEM); the domain size of the PA1010 dispersed phase in the HIPS matrix of compatibilized blends decreased comparing with that of uncompatibilized blends. For the blend with 25 wt % HIPS-*g*-MA component, the T_c of PA1010 shifts towards lower temperature, from 178 to 83°C. It is found that HIPS-*g*-MA used as the third component has profound effect on the mechanical properties of the resulting blends. This behavior has been attributed to the chemical reaction taking place *in situ* during the mixing between the two components of PA1010 and HIPS-*g*-MA. © 2000 John Wiley & Sons, Inc. *J Appl Polym Sci* 76: 799–806, 2000

Key words: polyamide 1010; high impact polystyrene; compatibilization

INTRODUCTION

Multicomponent materials are frequently made by blending two or more miscible or immiscible polymers. The mechanical blending of miscible polymers results in a homogeneous morphology that exhibits a single glass transition.¹ However, the mechanical blending of immiscible but compatible components, such as polycarbonate with acrylonitrile–butadienestyrene, gives a multiphase morphology with efficient dispersion of the minor component and good interfacial adhesion between the two unmodified components.² When incompatible thermoplastic polymers such as high impact polystyrene (HIPS) and polyamide1010 (PA) are mixed, the interfacial adhe-

sion is weak, which results in inferior mechanical properties and poor dispersion of the components. These blends require a compatibilizing agent to achieve satisfactory interfacial adhesion and interfacial stress transfer between the phases. One approach to polymer blend compatibilization is to manipulate the interactions at the interface by the addition of “interfacial agents” that facilitate graft reactions.³

For the polyamides/polyolefin systems, on the one hand, polyamides (PA) are frequently blended with lower modulus polymers such as rubbers⁴ or polyolefins⁵ to improve material properties. The addition of polyolefins lowers water absorption and reduces material cost. On the other hand, polyolefins are often blended with other polymers to improve its performance in specific applications. The addition of a PA serves to significantly increase the yield strength of the material if the components can be made to interact construc-

Correspondence to: J. Liu.

Journal of Applied Polymer Science, Vol. 76, 799–806 (2000)
© 2000 John Wiley & Sons, Inc.

tively. Functionalized polyolefin compatibilizers are popular third components that are added to aid both adhesion and mixing in the polyolefin/PA system. Compatibilizing agents for these blends have been developed by grafting maleic anhydride (MA) onto polyolefin chains where the amount of grafted anhydride can be varied.⁶ In PP/PA blends, the PP grafted maleic anhydride compatibilizer forms a chemical linkage through the reaction of anhydride groups with the end groups of polyamide. Consequently, a graft copolymer with segments of PP and PA is formed *in situ* at the interface. The graft copolymer improves interfacial compatibility by association of the different segments with their respective components. Because the compatibilizing process occurs by reactive mixing, special consideration must be given to the amount of maleic anhydride graft used in the compatibilizing agent. A similar reactive pattern should occur in the blends of the HIPS/PA/maleated grafting copolymer.

Our previous study⁷ has shown HIPS-*g*-MA to be an effective compatibilizer for 75PA1010/25HIPS blends. Compatibilization is considered to occur through a chemical linkage of the anhydride on the compatibilizer chain and the PA end groups. Model reactions of amines with anhydride-grafted HIPS at melt temperatures proceed to imide linkages, but it is difficult to determine the amide vs. imide structure in the PA/HIPS blends. The formation of the graft copolymer through the reaction of the anhydride with the polyamide end group has been confirmed through the change of morphologies and mechanical properties. The grafted copolymers preferentially reside at the interface and improve the dispersion, interfacial adhesion, and mechanical properties through the chemical linkage across the interface.

In general, this blend system, HIPS/PA1010, has important meaning both to scientific and commercial applications. As is well known, HIPS is a commercial product in large use. It has been used to manufacture refrigerator inner box, TV housing, etc., throughout the world. However, HIPS liners could meet problems in terms of the environment friendly blowing agents, HCFC-141b, from rigid polyurethane foam used for the insulation of domestic refrigerators and freezers. A new objective of this work was to investigate the foam/liner interactions, and ultimately develop a HCFC-141b-compatible liner. The compatibilized blends of HIPS and PA1010 have successfully been used to manufacture the liners of refrigerators and freezers with an HCFC-141b

blowing agent in China. From a scientific point of view, it is necessary to highlight the relationship among the miscibility, the effect of compatibilizer, morphology, and mechanical properties of the blends of HIPS and PA1010. The present study was aimed at understanding the relationship between the nature of the compatibilizer and the resulting blend morphology and properties. In particular, HIPS/PA1010 blends in which the HIPS is the rich phase were investigated by using two compatibilizers with widely different graft anhydride concentrations.

EXPERIMENTAL

Materials

HIPS employed in this study was a commercial grade (492-J) manufactured by the Yanshan Petrochemical Co. Beijing, China. Polybutadiene (7%) was utilized during the polymerization of HIPS. Its MFR was 2.6 g/10 min. PA1010 was supplied from Jilin Shijinggou Union Chemical Co., China. Its relative viscosity was 2.1, and the melting flow rate was 10 g/10 min.

Preparation of Compatibilizer and Blends

HIPS-*g*-MA was prepared by melt mixing initiated by dicumyl peroxide (DCP) in a Brabender mixing chamber. The mixing temperature was controlled at 180°C. The content of MA in HIPS-*g*-MA used in this work was 1.6 wt % (LMA) and 4.7 wt % (HMA), respectively. The grafting degrees were determined by the chemical titration method.

PA1010 was dried for 24 h at 90°C before melt blending. The ternary blends, HIPS/PA1010/HIPS-*g*-MA, were prepared by melt mixing using a Brabender mixer operating at a rotation speed of 50 rpm and mixing temperature designed as 200–210°C. The amount of HIPS in the blend was adjusted so that the total amount of HIPS and HIPS-*g*-MA was 75 wt %, while the PA1010 remained constant at 25% by weight. The amount of HIPS-*g*-MA (HMA or LMA) in the blends was 2.5, 5, and 10 wt % of the total blend weight.

Morphological Observation

The morphology of blends was observed with a scanning electron microscope (SEM, JXA-840) at an accelerating voltage of 25 kV. The blend samples were fractured at liquid nitrogen tempera-

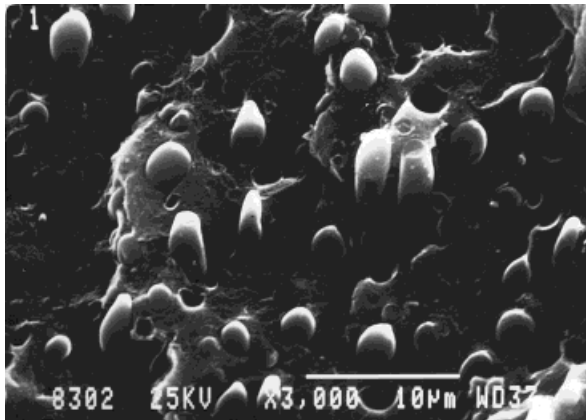


Figure 1 SEM micrographs of fractured surface of a HIPS/PA1010 75/25 blend.

ture, and the cryogenically fractured samples etched with formic acid (a good solvent for polyamide) to increase the contrast.

Crystallization and Thermal Analysis

The thermal behavior of blended samples was determined on a Perkin-Elmer DSC-7. The fusion thermal curve was obtained from 50 to 220°C at a heating rate of 20°C/min. All measurements were performed under a nitrogen atmosphere.

Tensile Properties

Dumb bell-shaped specimens were prepared at 230°C with hot-press molding. The tensile tests were carried out on an Instron 1121 machine at 23°C with a crosshead speed of 5 mm/min. Five specimens of each blend were tested and average values were taken as experimental data.

RESULTS AND DISCUSSION

Morphology

The uncompatibilized blend of HIPS/PA1010 (75/25) had a coarse morphology, with a domain sizes as large as 3 μm (Fig. 1). The large voids left on the fracture surface where the particles had separated from the matrix and the smooth surfaces of the exposed PA particles, with no evidence of adhesion between the matrix and dispersed phase, confirmed the immiscibility of the two components. In compatibilized blends, the PA was dispersed in the HIPS as spherical particles. The addition of 5 wt % LMA reduced the average

particle size in the blends to 0.8 μm [Fig. 2(a)]. However, the average particle size is reduced to 0.6 μm by addition of 5 wt % HMA [Fig. 2(c)]. Interfacial adhesion also seemed to be improved with addition of a 5 wt % compatibilizer because some of the PA particles on the fracture surfaces had been adhered with the matrix material. Better dispersion and improved interfacial adhesion were attributed to formation of a HIPS-g-MA/PA copolymer by reaction of anhydride groups with terminal amine groups of PA during melt mixing. The dispersion was improved when the copolymer stabilized the interface by forming an interfacial layer between PA1010 particles and the HIPS matrix. Improved adhesion depended on strong chemical or physical interactions between particles and matrix. The blends with 5 and 10 wt % HMA, are shown in Figure 2(c) and (d). The micrographs illustrate the reduction in particle size with increasing compatibilizer content, and also suggest better adhesion in the blend with higher compatibilizer content because the particles in the 10 wt % HMA blend appear to be more deeply embedded in the matrix. A morphology gradient was especially apparent in the blend with a lower compatibilizer content.

The average particle size of dispersed phase is plotted in Figure 3 as a function of the amount of compatibilizer. It shows that the particle size depended on the amount of compatibilizer, but was not strongly affected by HMA or LMA used in the blends. Small concentrations of a compatibilizer of LMA had a very large effect on particle size, for example, 2.5 wt % LMA decreased the average particle size from over 2.4 μm to less than 1.0 μm. Further increases on anhydride concentration, up to 10 wt % resulted in only minimal additional decrease in particle size. To the blends with HMA, the smallest amount of HMA used, 2.5 wt %, was sufficient to achieve a PA particle size less than 0.8 μm. To achieve a PA particle size less than 0.6 μm with HMA, 10 wt % of the compatibilizer was necessary.

If it is assumed that the graft copolymer is located at the interface between the two phases with complete penetration of the two phases, the interfacial area stabilized per molecule (A) can be estimated by

$$A = \frac{3\phi M_n}{RW_c N} \quad (1)$$

where ϕ is the volume fraction of the dispersed phase, M_n is the number-average molecular

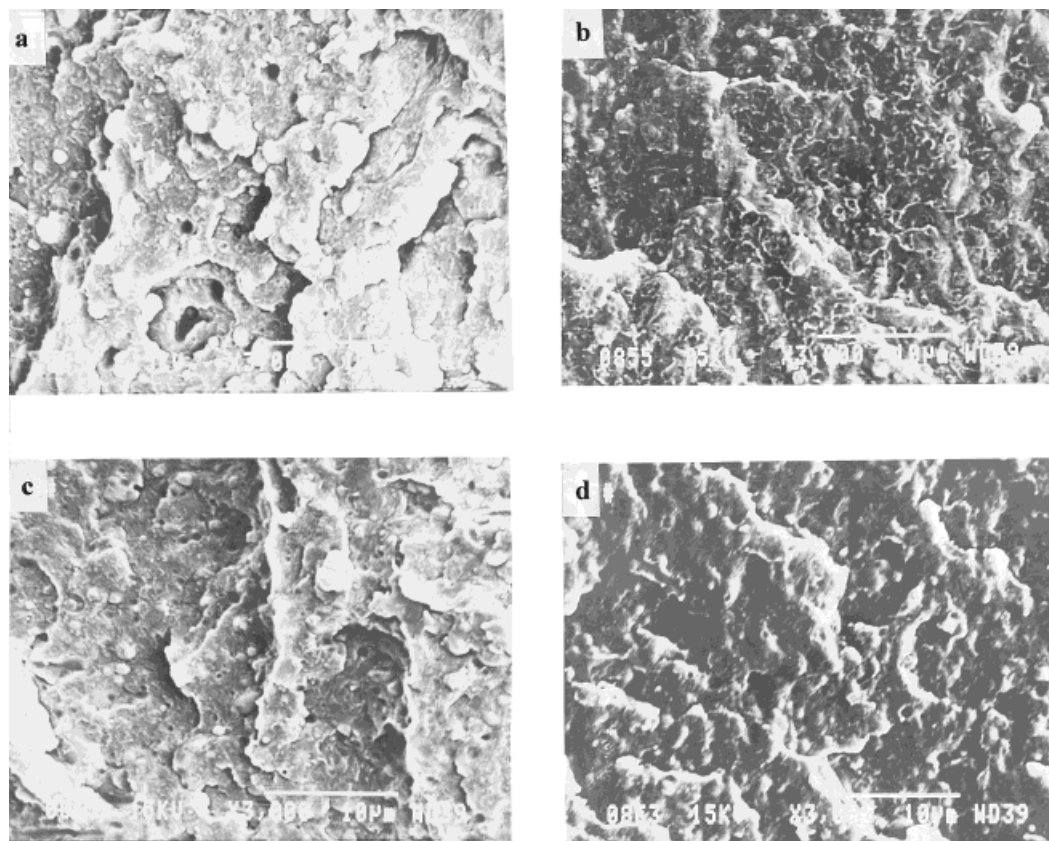


Figure 2 SEM micrographs for 25 wt % PA1010 blends containing: (a) 5 wt % LMA, (b) 10 wt % LMA, (c) 5 wt % HMA, (d) 10 wt % HMA.

weight of the compatibilizer, R is the particle radius, W_c is the mass of compatibilizer per unit volume of blend, and N is Avogadro's number, respectively. For the systems used, M_n and N can be regarded as the constant parameter. The calculated values of surface area stabilized per compatibilizer molecule are estimated in Table I. With this qualification, the average interfacial area per compatibilizer molecule is remarkably similar for LMA and HMA, and is not strongly affected by compatibilizer content. However, the calculation assumed that all compatibilizer stabilized at the interface was needed in the subsequent interpretation of these numbers.

Crystallization and Thermal Analysis

The differential scanning calorimetric (DSC) thermal curves of HIPS/PA1010/HIPS-*g*-MA blends and neat PA1010 were shown in Figure 4. The heat of fusion of PA1010 at lower temperature has decreased as HIPS-*g*-MA increased, and the T_m of PA1010 at a higher temperature is

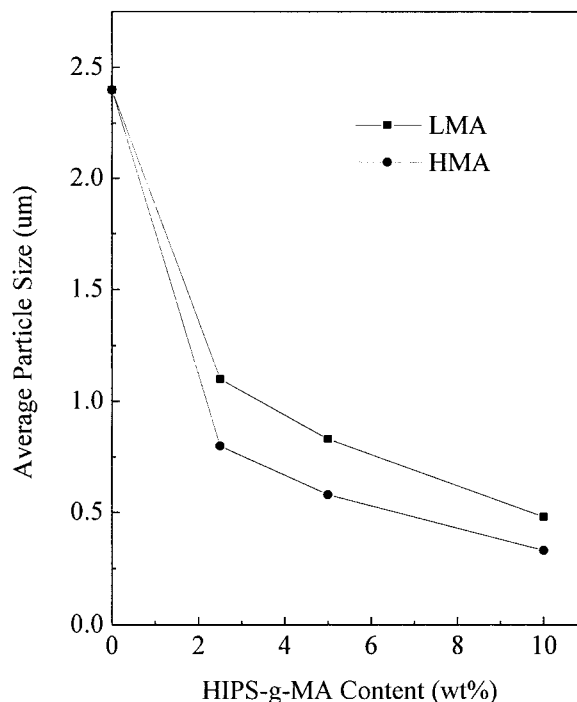
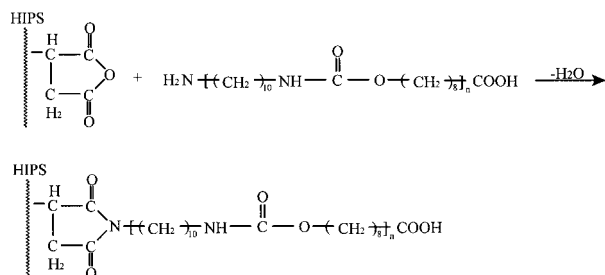


Figure 3 Average PA1010 particle size as a function of HIPS-*g*-MA content: 2.5, 5, and 10 wt %.

Table I Surface Areas Stabilized per Molecule of Compatibilizer

HIPS- <i>g</i> -MA Content (wt %)	A-LMA ($\times M_n/N$)	A-HMA ($\times M_n/N$)
2.5	30.0	41.1
5	21.7	31.0
10	21.9	31.8

unaffected by adding HIPS-*g*-MA. This feature suggests that some chemical reaction occurred between the MA groups in HIPS-*g*-MA and terminal amino group of PA1010 in the HIPS/PA1010/HIPS-*g*-MA blend as follows:



The variation of the double-melting behavior of PA66 on the DSC curve of PA66/PEI blends is also found, and the heat of fusion of the lower endotherm is found to change with the T_c .⁸ It seems that the crystals formed at a lower T_c usually contain a bit of smaller and more defective

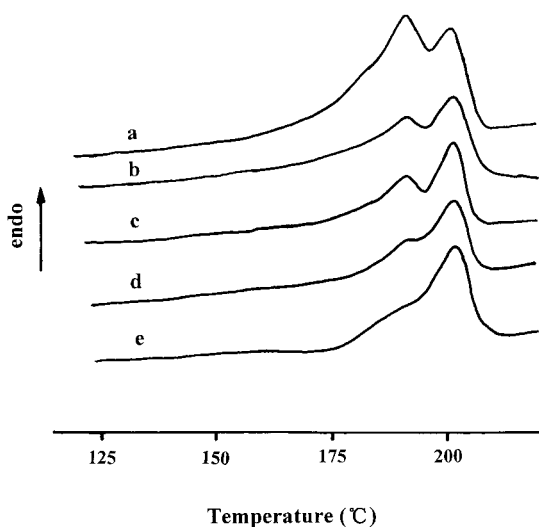


Figure 4 DSC curves of PA1010 (a) and HIPS/PA1010/HMA blends: (b) 75/25/0, (c) 70/25/5/, (d) 65/25/10, (e) 50/25/25.

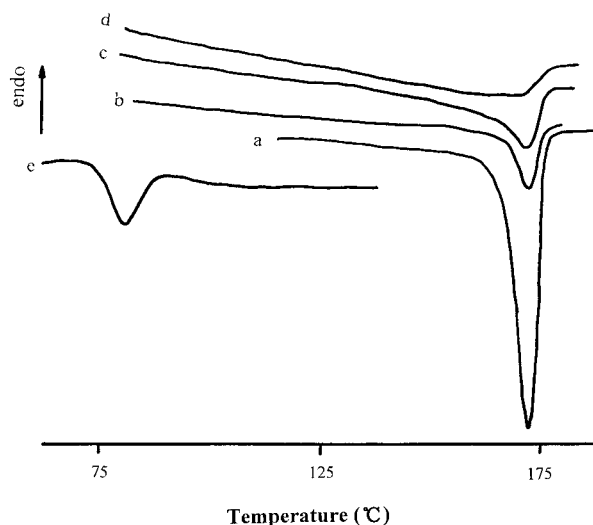


Figure 5 DSC crystallization curves of PA1010 (a) and HIPS/PA1010/HMA blends: (b) 75/25/0, (c) 70/25/5, (d) 65/25/10, (e) 50/25/25.

spherulites. Perhaps most of them are positive spherulites with branched fibril structure. After the initial melting, these crystalline domains may still exhibit large mobility and sufficient molecular ordering that would facilitate the reorganization process. In contrast, the crystals formed at higher T_c are larger, and perfect positive spherulites that may lead to a lower mobility upon pre-melting that often hinders the reorganization ability. These indicate that the crystals at lower temperature are less stable than that at a higher temperature, and this would be influenced by many factors such as T_c , heating speed, and the interaction of groups in material. In our system, the number of hydrogen bonds in the PA1010 phase decreased, owing to the chemical reaction. The big imide groups synthesized *in situ* between terminal amino group in PA1010 and MA groups in HIPS-*g*-MA can inhibit the fold of PA1010 molecular chains effectively, so the heat of fusion of PA1010 at a lower temperature decreased. For the higher temperature peaks, the heat of fusion of PA1010 has no changes because of the reorganization of PA1010, while the other molecular impurities could be removed from the crystalline phase of PA1010.

The DSC cooling curves of the blends of HIPS/PA1010/HIPS-*g*-MA and PA1010 are shown in Figure 5. The crystallization peak is broader with the increase of the HIPS-*g*-MA component. For the blend with 25 wt % of the HIPS-*g*-MA component, the T_c of PA1010 shifts towards a lower

temperature, from 178 to 83°C. This so-called fractionated crystallization is observed. The described effects, in particular the fractionation of the crystallization, depend to a large extent on the dispersion of the minor component. With increasing dispersivity of that component, the magnitudes of its additional crystallization peaks become stronger at the expense of the usual peak.

The fractionated crystallization is characteristic of the crystallization behavior of a semicrystalline polymer blended with an immiscible polymer. This phenomenon has been observed so far in block copolymers comprising PEO-PS^{9, 10} and in blends comprised of PE/PS,¹¹ PVDF/PA6,¹² PA6/PP,¹³ PBT/PC,¹⁴ and PA/ABS¹⁵ when the crystallizable component is included in the non-crystallizable matrix in finely dispersed domains. The smaller the particles, the more distinct is the effect.

Among a larger amount of small polymer droplets each of volume V_D , the fraction of droplets containing exactly Z heterogeneities of the kind "1" that initially induced crystallization follows a Poisson distribution function.¹⁶ It reads:

$$f_z^{(1)} = [(M^{(1)}V_D)^Z/Z!]\exp(-M^{(1)}V_D) \quad (2)$$

where $M^{(1)}$ is the concentration of randomly suspended heterogeneities, and $M^{(1)}V_D$ is their mean number per droplet. The fraction of droplets containing at least one heterogeneity of the kind "1" is given by $f_{z>0}^{(1)} = 1 - f_0^{(1)}$, and amounts to

$$f_{z>0}^{(1)} = 1 - \exp(-M^{(1)}V_D) \quad (3)$$

The consideration of a droplet size distribution may somewhat modify this equation. $f_{z>0}^{(1)}$ describes that part of the droplets and, therefore, of the material that crystallizes induced by heterogeneity "1." The remainder crystallizes at a greater undercooling degree induced by heterogeneity "2," and so on. For these further crystallization steps the same considerations hold. Because $f_{z>0}^{(i)}$ depends on V_D , the influence of the dispersivity on the relative strength of the different crystallization steps is obvious. For sufficiently large droplets, $f_{z>0}^{(1)}$ is near unity, and no fractionated crystallization occurs. On the contrary, a certain crystallization step is suppressed (or undetectable) if the relation $M^{(i)}V_D \ll 1$ holds. From the relative intensity of the different crystallization steps, conclusions can be drawn on the concentration of the respective heterogeneities if

the mean size of the droplets is known. From the results shown in Figure 5, we can conclude that the domain size, that is V_D , in the HIPS/PA1010/HIPS-*g*-MA (50/25/25) blend is small enough so that the fractionated crystallization in the PA1010 phase was obviously detected. On the other hand, the fractionated crystallization of PA1010 domains in PA1010/HIPS blends cannot be observed at all. This is related to the larger volume of droplets in these blends. These results deal with the micrographs of the samples shown in Figure 2.

Morphology generation during mixing of polymer components involves a balance between the competing processes of fluid drop breakup and coalescence. Taylor studied the deformation and disintegration of Newtonian fluids.^{17,18} Tokita has derived an expression for describing the particle size of a dispersed phase in polymer blends.^{18,19} At equilibrium, where breakup and coalescence are balanced, the equilibrium particle size, D , may be expressed as:

$$D = (24P_r\nu/\pi\sigma_{12})(\Phi + 4P_rE\Phi^2/\pi\sigma_{12}) \quad (4)$$

where σ_{12} , ν , E , and P_r refer to stress field, interfacial tension, bulk breaking energy, and probability that a collision will result in coalescence, respectively. Equation (4) predicts that the equilibrium particle size decreases when the stress field becomes larger, the interfacial tension becomes smaller and the volume fraction of the dispersed phase is smaller. As represented in Figure 3, because the decrease of the interfacial tension resulted from the chemical reaction between the components of PA1010 and HIPS-*g*-MA, the average domain size was reduced to approximately 1/20, compared with those in the uncompatibilized blend systems at the same composition. These results are in agreement with the trends predicted in eq. (4). The average volumes, V_D , of the dispersed PA1010 particles in the HIPS/PA1010/HIPS-*g*-MA 50/25/25 blend is significant smaller than those in the system of HIPS/PA1010/HIPS-*g*-MA with other compositions, so that the relation $M^{(i)}V_D \ll 1$ holds, and the fractionated crystallization is observed.

Tensile Properties

Figure 7 shows the effect of compatibilizer on the tensile strength of HIPS/PA1010 blends containing a 25 wt % PA1010 component. The addition of a compatibilizer increased the tensile strength

from 24.8 MPa in the uncompatibilized blend to 30.2–31.1 MPa, which was also higher than the HIPS control (25.5 MPa). The low tensile properties of the HIPS/PA1010 blend can be essentially related to the larger size of the PA1010 domains with a poor adhesion to the matrix. These domains act as gross material defects, causing premature rupture of the specimen soon after the beginning of yield. On the other hand, the improvement of tensile strength was attributed to improved adhesion and homogeneity and decreased particle size in the compatibilized blends that facilitated stress transfer of the PA particles and increased their load-bearing capacity. From the morphological observation, we realized that the PA1010-*g*-HIPS copolymer, which was formed during melt mixing, improved the tensile properties of the HIPS/PA1010 blends.

Tensile strength of the LMA-compatibilized blends increased from 28.5 to 29.8 and 30.2 MPa with increasing the compatibilizer from 2.5 to 5 and 10 wt %, while the blends with HMA had the strength of 29.5, 30.2 and 31.1 MPa. The tensile strength was similar in HMA and LMA blends because adhesion was maintained until the matrix yielded. The elongation at break gradually increased as the LMA content increased from 5 to 10 wt %, and the better adhesion provided by LMA was manifest primarily in the ultimate elongation. The increased tensile strength of all the compatibilized blends suggested that the interfacial strength can be improved sufficiently to inhibit particle debonding before yielding, even though the smallest amount of compatibilizer was

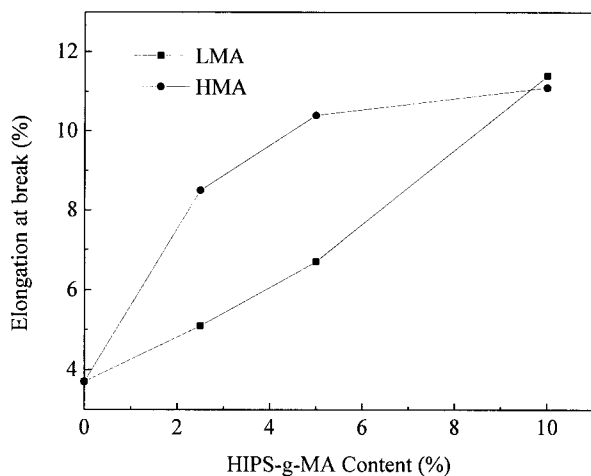


Figure 6 Tensile strength as a function of HIPS-*g*-MA weight percent for HIPS/PA1010/HIPS-*g*-MA blends: 75/25/0, 72.5/25/2.5, 70/25/5, and 65/25/10.

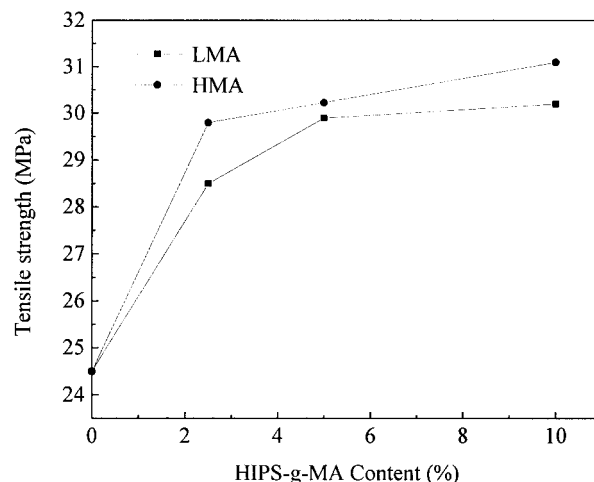


Figure 7 Elongation at break as a function of HIPS-*g*-MA weight percent for HIPS/PA1010/HIPS-*g*-MA blends: 75/25/0, 72.5/25/2.5, 70/25/5, and 65/25/10.

added. However, debonding of the PA particles during yielding was indicated in the blends with a 5 wt % compatibilizer by the low elongation, comparable to the elongation of the uncompatibilized blend. The gradually increasing elongation at break with increasing the compatibilizer content was attributed to improved interfacial strength.

CONCLUSIONS

Binary blends of the HIPS and PA1010 copolymer were immiscible with poor interfacial adhesion and large-phase domains. In compatibilized ternary blends, chemical reaction took place between the anhydride groups in the HIPS-*g*-MA and terminal amino groups of PA1010, and increased the adhesion between two phases. Both a low-anhydride compatibilizer and a high-anhydride compatibilizer improved the dispersion of PA1010 in HIPS matrix. For the blend with a 25 wt % HIPS-*g*-MA component, the so-called fractionated crystallization was observed. The tensile strength of the uncompatibilized blend was lower than that of HIPS due to poor adhesion between the phases. With improved adhesion, the tensile strength of the compatibilized blends was about twice of the uncompatibilized blend, and was also higher than that of HIPS. No remarkable difference was detected on the tensile strength of the compatibilized blends by using LMA and HMA.

REFERENCES

1. Stoelting, J.; Karasz, F. E.; Macknight, W. J. *Polym Eng Sci* 1970, 10, 133.

2. Kurauchi, T.; Ohta, T. *J Mater Sci* 1984, 19, 1699.
3. Paul, D. R.; Newman, S., Eds. *Polymer Blends*; Academic Press: New York, 1978.
4. Takeda, Y.; Keskkula, H.; Paul, D. R. *Polymer* 1992, 33, 3173.
5. Padwa, A. R. *Polym Eng Sci* 1992, 32, 1703.
6. Gaylord, N. *J Polym Sci Polym Lett Ed* 1983, 21, 23.
7. Chen, G. X.; Yang, J.; Liu, J. J. *J Appl Polym Sci* 1999, 71, 2017.
8. Lee, J. H.; Lee, S. G.; Choi, K. Y.; Liu, J. *Polym J* 1998, 7, 531.
9. Lotz, B.; Kovacs, A. J. *Polym Prep* 1969, 10, 820.
10. Robitaille, V. I. *Prudomme, J. Macromolecules* 1983, 16, 665.
11. Aref-Azar, A.; Hay, J. N.; Marsden, B.; Neil, W. *J Polym Sci Polym Phys* 1980, 18, 637.
12. Frensch, H.; Jungnickel, B. *J. Colloid Polym Sci* 1989, 28, 2267.
13. Ikkala, O. T.; Holsti-Miettinen, R. M.; Seppala, J. *J Appl Polym Sci* 1993, 49, 65.
14. Radusch, H.-J.; Androsch, R. *Angew Makrom Chem* 1994, 214, 179.
15. Stolp, M.; Androsch, R.; Radrsch, H.-J. *Polym Networks Blends* 1996, 4, 1141.
16. Pound, G. M.; Lamer, V. K. *J Am Chem Soc* 1952, 74, 2323.
17. Taylor, G. I. *Proc R Soc Lond* 1934, A146, 501.
18. Taylor, G. I. *Proc R Soc Lond* 1932, A138, 41.
19. Todita, N. *Rubber Chem Technol* 1977, 50, 292.